Acoustic Diagnostics of Plasma Channels Induced by Intense Femtosecond Laser Pulses in Air

2005 Chinese Phys. Lett. 22 636

(http://iopscience.iop.org/0256-307X/22/3/032)

Acoustic Diagnostics of Plasma Channels Induced by Intense Femtosecond Laser Pulses in Air *

HAO Zuo-Qiang(郝作强)[1], YU Jin(俞进)[2], ZHANG Jie(张杰)[1**], LI Yu-Tong(李玉同)[1], YUAN Xiao-Hui(远晓辉)[1,3], ZHENG Zhi-Yuan(郑志远)[1], WANG Peng(王鹏)[1], WANG Zhao-Hua(王兆华)[1], LING Wei-Jun(令维军)[1], WEI Zhi-Yi(魏志义)[1]

[1]*Laboratory of Optical Physics, Institute of Physics, Chinese Academy of Sciences, Beijing 100080*

[2]*Laboratoire de Spectroétrie Ionique et Moléculaire, UMR CNRS 5579, Université Claude Bernard-Lyon 1,43, Bd. du 11 Novembre 1918, F-69622 Villeurbanne Cedex, France*

[3]*State Key Laboratory of Transient Optics Technology, Xi'an Institute of Optics and Precision Mechanics, Chinese Academy of Sciences, Xian 710068*

(Received 29 October 2004)

Long plasma channels induced by femtosecond laser pulses in air are diagnosed using the sonographic method. By detecting the sound signals along the channels, the length and the electron density of the channels are measured. Refocusing is also observed at different laser energies and different focal lengths. We find that the sonographic method has manifest advantages compared to other techniques.

PACS: 52. 38. Hb, 52. 35. Hp

In recent years, there has been great interest in the formation of long plasma channels in air induced by femtosecond laser pulses.[1−9] The fundamental mechanism is the dynamic balance between the nonlinear Kerr self-focusing due to nonlinear intensity-dependent refractive index and plasma defocusing due to high-order multiphoton ionization (MPI) of air and the normal diffraction of the laser beam. The plasma channels propagate up to thousands of metres in the atmosphere,[3] exceeding many Rayleigh lengths of the laser beam. The intensity of the laser beam in the channels is typically about 5×10^{13}–$1 \times 10^{14}\,\mathrm{W/cm^2}$,[10] and the electron density in the channels can reach $10^{18}\,\mathrm{cm^{-3}}$.[11] It is difficult to directly measure the intensity distribution in the channels. Some methods have been used to diagnose the plasma channels, such as shadowgraphy,[12,13] interferometry,[10,11] electric conductivity method,[4−6,14] fluorescence detection,[15−19] and so on. These methods have their own advantages and drawbacks. In this Letter, we use the sonographic method[20] to measure the length and the gross intensity distribution in the channels as well as the electron density in the plasma channels. This diagnostic method has many advantages compared with other ones.

Figure 1 shows the experimental setup. The laser system is a home-made Ti:sapphire chirped-pulse amplification system (JG-Ⅱ) with an output energy up to 640 mJ in 30 fs pulses at a central wavelength of 800 nm. The repetition rate is 10 Hz. At the output of the compressor chamber, the beam profile is nearly Gaussian. The initial laser beam waist radius ω_0 is about 1.5 cm. In our experiments, we produce long plasma channels propagating many Rayleigh lengths. The channels can be seen directly by the naked eye. A microphone is placed perpendicularly to the channels at a distance of 7 cm from the laser axis. The sound signals are recorded by a digital oscilloscope after being amplified by an audio amplifier.

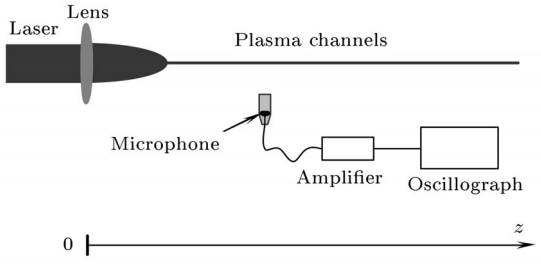

Fig. 1. Schematic diagram of the experimental setup.

The microphone output voltage as a function of the propagation distance is shown in Fig. 2. The energy of the laser pulse is set to be 39 mJ (Fig. 2(a)) and 50 mJ (Fig. 2(b)) respectively. The focal length of the positive lens used is $f = 4$ m. However, the best geometrical focus locates at 506 cm because the laser beam we used in experiments has a divergence angle. We can see changes in the sound signals by changing the distance of the microphone along the plasma channels. Higher amplitude signals represent higher

* Supported by the National Natural Science Foundation of China under Grant Nos 10176034, 10374116, 10390160, and 60478047, the National Key Basic Research Special Foundation of China under Grant No G1999075206, and the National Hi-Tech ICF Programme.

** To whom correspondence should be addressed. Email: jzhang@aphy.iphy.ac.cn

free- electron density inside the plasma channels. In order to reduce background noise, the laser pulse fluctuations and air turbulence, the signals are averaged over 200 laser pulses. In Fig. 2, the rapid increase of the signal around 420 cm in Fig. 2(a) and 380 cm in Fig. 2(b) indicates the starting of the plasma channels, and the rapid decrease around 542 cm in Fig. 2(a) and 550 cm in Fig. 2(b) indicates the ending of the filaments as pointed to by arrows. This indicates that the length of the channels is at least 122 cm for laser pulse energy of 39 mJ and 170 cm for the energy of 50 mJ. We also detect the sound signals of the plasma channels using an $f = 8$ m lens for a laser energy of 50 mJ. The corresponding geometrical focal length is 1810 cm. The result is shown in Fig. 3. We can conclude that the intense femtosecond laser pulse can form long plasma channels.

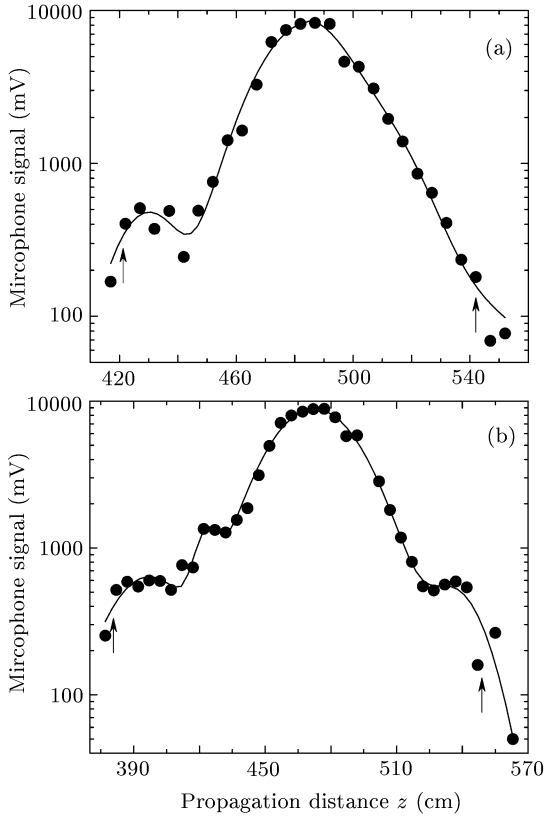

Fig. 2. Peak sound signals versus propagation distance. The energy of laser pulse is 39 mJ (a), and 50 mJ (b) respectively. The focal length of the lens used is 4 m.

Assuming the collimated beam focused with a lens $f = 4$ m in our experiments, we obtain its Rayleigh length as $z_f = z_0 f^2/z_0 f^2(z_0^2 + f^2) \sim 1.8$ cm, where $z_0 = \pi\omega_0^2 la \sim 883.6$ m is the diffraction length of the collimated beam. We can see that the plasma channel propagates over several tens of Rayleigh lengths in our experiments. Under the condition of lens $f = 8$ m, $z_f \sim 7.24$ cm, therefore we obtain the plasma channel with about 100 Rayleigh lengths.

The long plasma channels can be formed by intense femtosecond laser pulses in air. In the channels, air molecules are partially ionized through the multiphoton ionization instantly by intense laser pulses. Plasma shock waves are formed and then decay to plasma sound wave subsequently, which are the sound signals we detect in the experiments. It has been found that the intensity of sound wave is related with the free-electron density in the plasma.[21]

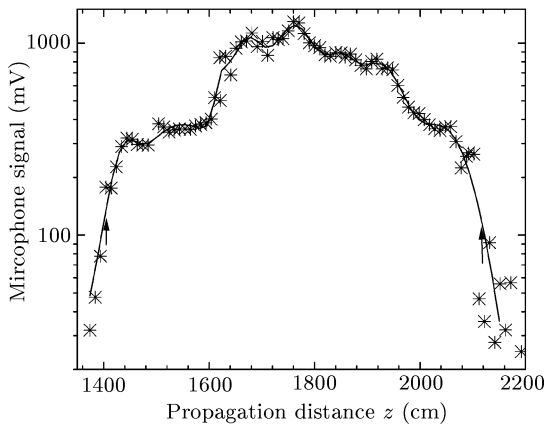

Fig. 3. Peak sound signals versus propagation distance. The focal length of the lens is 8 m and the laser energy is 50 mJ.

Free-electrons in plasma channels mainly come from oxygen and nitrogen molecules. Therefore, electron density growth rate in the channels at a distance z is expressed as[13]

$$\begin{aligned} dN_e(z,t)/dt &= R(I) \times N(z) \\ &= R_{\mathrm{N_2}}(I) \times N_{\mathrm{N_2}} + R_{\mathrm{O_2}}(I) \times N_{\mathrm{O_2}}, \end{aligned} \tag{1}$$

where $N_{\mathrm{N_2}}$ and $N_{\mathrm{O_2}}$ represent the density of nitrogen and oxygen in air respectively, $R(I)_{\mathrm{N_2}}$ and $R(I)_{\mathrm{O_2}}$ are the corresponding electron generation rate that will increase exponentially with the laser intensity:[22,23]

$$R(I)_{\mathrm{N_2/O_2}} = R_{\mathrm{T,N_2/O_2}} \times [I(z,t)/I_T]^{\alpha_{\mathrm{N_2/O_2}}}, \tag{2}$$

where R and I_T are experimental values used as a reference point and α is a linear fit slope.

In the channels, free electrons absorb laser energy by the process of inverse bremsstrahlung. The rate of kinetic energy growth of electrons is given by[24]

$$\frac{dE_e(z,t)}{dt} = \frac{e^2\nu_{\mathrm{eff}}}{m\omega^2}\frac{2I(z,t)}{\varepsilon_0 c} \times N_e(z,t) \times \pi\left[\frac{\phi(z)}{2}\right]^2 l, \tag{3}$$

where e is the electron charge, ν_{eff} is the effective collision frequency between free electrons and molecules; $\phi(z)$ and l are the diameter and length of the channel. Then, the energy of electrons in the channels is

$$E_e(z) = \frac{e^2\nu_{\mathrm{eff}}}{m\omega^2}\int_{-\infty}^{+\infty}\frac{2I(z,t)}{\varepsilon_0 c}dt$$

$$\times \int_{-\infty}^{t} N_e(z,t')dt' \times \pi\Big[\frac{\phi(z)}{2}\Big]^2 l$$
$$= \frac{e^2\nu_{\rm eff}}{m\omega^2}\frac{2}{\varepsilon_0 c}\pi\Big[\frac{\phi(z)}{2}\Big]^2 l \times \int_{-\infty}^{+\infty} I(z,t)dt$$
$$\times \int_{-\infty}^{t} \Big\{R_{\rm T,N_2}\Big[\frac{I(z,t')}{I_T}\Big]^{\alpha_{\rm N_2}} N_{\rm N_2}$$
$$+ R_{\rm T,O_2}\Big[\frac{I(z,t')}{I_T}\Big]^{\alpha_{\rm O_2}} N_{\rm O_2}\Big\}dt'. \quad (4)$$

The sound emitted from plasma channels is a portion of the pressure modulation due to the acoustic wave: $S(t) = A\times p_0 f(t)$, where A is the gain of the detection, p_0 is the amplitude of the pressure wave, and $f(t)$ is its temporal form. Because of the small area of the detecting head of the microphone, the spherical wave front of the sound can be approximated to a plane wave. Therefore, the sound intensity formula can be used, $J(t) = p^2(t)/(2\rho_0 c_0)$, where ρ_0 is the density of air, and c_0 is the acoustic wave phase velocity. The energy of sound wave of a segment of filament with length l is related to microphone signal by

$$E_a(z) = 2\pi Rl \times \int_{-\infty}^{+\infty} J(t)dt$$
$$= \frac{2\pi Rl}{2\rho_0 c_0} \times \int_{-\infty}^{+\infty} p^2(t)dt$$
$$= \frac{2\pi Rl}{2\rho_0 c_0} \times \Big(\frac{S_0(z)}{A}\Big)^2 \int_{-\infty}^{+\infty} f^2(t)dt$$
$$= \frac{\pi Rl}{\rho_0 c_0} \times \frac{S_0^2(z)}{A^2} \int_{-\infty}^{+\infty} f^2(t)dt, \quad (5)$$

where $S_0(z)$ is the detected peak voltage signal at z, and R is the distance of the microphone from the channels.

The sound energy is proportional to the absorbed optical energy.[25] We use a partition factor $\gamma(\gamma < 1)$: $E_a = \gamma E_e$ to connect them. Finally the peak sound signal is related to the light intensity of the channel by

$$S_0(z) = C\sqrt{E_e(z)}, \quad (6)$$

where C is a constant given by

$$C = \sqrt{\gamma A^2\Big[\frac{\pi Rl}{\rho_0 c_0}\int_{-\infty}^{+\infty} f^2(t)dt\Big]^{-1}}.$$

Therefore, the distribution of electron density along the plasma channels can be obtained by use of the model mentioned above. The laser beam used is a Gaussian profile pulse approximately, $I(z,t) = I_0(z)\exp[-(t/t_0)^2]$. We take the maximum free electron density with the value of $2.7\times10^{18}\,\mathrm{cm}^{-2}$ obtained by Yang *et al.*[11] in order to calibrate our microphone. Furthermore, we assume that the intensity of plasma channels only depends on the diameter of channels because of the clamping effects of the laser intensity in channels. Then we calculate [using Eqs. (4) and (6)] the intensities and diameters of the channels as functions of the propagation distance. The calculated intensities are in turn substituted into Eqs. (1)–(3) to calculate the electron density profile along the channels.

In the calculation, the parameters are taken from Ref. [23]:

(a) $I_T = 10^{14}\,\mathrm{W/cm^2}$,
$R_{\rm T,N_2} = 10^{12}\,\mathrm{s^{-1}}$,
$\alpha_{\rm N_2} = 4.2$,
$R_{\rm T,O_2} = 3.6\times10^{12}\mathrm{s^{-1}}$
and $\alpha_{\rm O_2} = 3.7$
when $I \geq 10^{14}\,\mathrm{W/cm^2}$;

(b) $I_T = 10^{13}\,\mathrm{W/cm^2}$, $R_{\rm T,N_2} = 2.5\times10^4\,\mathrm{s^{-1}}$, $\alpha_{\rm N_2} = 7.5$ and

$$R_{\rm T,O_2} = \begin{cases} 5.6\times10^8, \alpha_{\rm O_2} = 3.8, \\ \text{for } 7\times10^{13}\,W/\mathrm{cm^2} \leq I < 10^{14}\,\mathrm{W/cm^2}, \\ 2.8\times10^6, \alpha_{\rm O_2} = 6.5, \\ \text{for } I < 7\times10^{13}\,\mathrm{W/cm^2}. \end{cases}$$

Also, the calculations are performed under the standard air conditions: $N_{\rm N_2} = 2\times10^{19}\,\mathrm{cm^{-3}}$, $N_{\rm O_2} = 5\times10^{18}\,\mathrm{cm^{-3}}$.

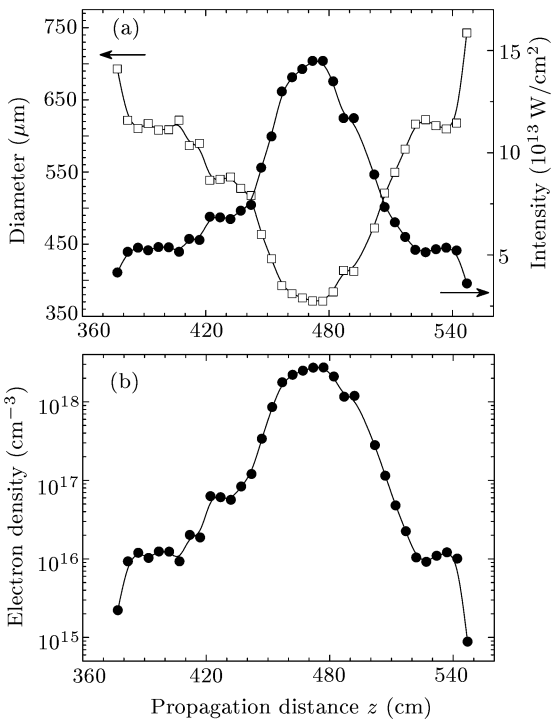

Fig. 4. Calculation results corresponding to Fig. 2(b): filaments diameter and filaments intensity (a) and electron density (b) versus the propagation distance.

The calculated channel diameter, channel intensity and electron density versus the propagation distance are shown in Fig. 4 for $f = 4\,\mathrm{m}$ and 50 mJ pulse en-

ergy. The maximum electron density in Fig. 4(b) leads to a minimum channel diameter of 370 μm as shown in Fig. 4(a). We can see from Fig.s 2(b) and 4(b) that the sound signal is proportional to the initial free-electron density generated by the MPI.[20]

Furthermore, we can see from Figs. 2 and 3 that the simple and multiple refocusings occur. The data is fitted by double-Gaussian graph in Fig. 2(a), four-Gaussian graph in Fig. 2(b) and seven-Gaussian graph in Fig. 3. The humps of the profile of the sound signals represent refocusing. The higher the laser pulse energy is, the more complicated the multiple refocusing is. The phenomenon can be explained by the moving focus model.[26–28]

Finally, in order to obtain characteristics of the sonographic method, we make a comparison among some existing experimental results measured by different methods. We can see from Figs. 4(b) and 2 that the electron density and sound profile are quite similar to the N_2^+ density profile measured by Proulx *et al.*[29] and the electromagnetic pulse (EMP) radiation profile detected by Hosseini *et al.*[30] This proves that the acoustic diagnostics method is reliable. However, the EMP detection is limited by the sensitivity of the wire detector and background electromagnetic radiation. Furthermore, Hosseini *et al.*[31] have also made a comparative study among three different methods, including electromagnetic pulse detection, backward propagating fluorescence (BF) and acoustic wave (AW) measurement. They concluded that the AW method is the most precise one compared to the other two methods. The sonographic measurement is a simple and robust method with a high sensibility and good spatial resolution.

In conclusion, we have probed the plasma channels in air generated by intense femtosecond laser pulses using the acoustic method. By measuring the sound signals along the channels, the channel length and distribution of electron density along the channel can be obtained conveniently, and the refocusing effects are also observed in the same time. The acoustic method has many advantages compared to other different methods. This method provides a convenient approach to detect long plasma channels nondestructively.

References

[1] Braun A et al 1995 *Opt. Lett.* **20** 73
[2] Yang H et al 2001 *Phys. Rev.* E **65** 016406
[3] Wöste L et al 1997 *Las. Optoelektron.* **29** 51
[4] Schillinger H and Sauerbrey R 1999 *Appl. Phys.* B **68** 753
[5] Tzortzakis S et al 1999 *Phys. Rev.* E **60** 3505
[6] Ladouceur H D et al 2001 *Opt. Lett.* **189** 107
[7] Bergé L et al 2004 *Phys. Rev. Lett.* **92** 225002
[8] Yang H, Zhang J et al 2003 *Phys. Rev.* E **67** 015401
[9] Kasparian J et al 2003 *Science* 301 61
[10] Fontaine B La et al 1999 *Phys. Plasmas* **6** 1615
[11] Yang H Zhang J et al 2002 *Phys. Rev.* E **66** 016406
[12] Liu W et al 2003 *Chin. Opt. Lett.* **1** 56
[13] Talebpour S et al 2000 *Opt. Commun.* **181** 123
[14] Tzortzakis S et al 2003 *Appl. Phys.* B **76** 609
[15] Yu J et al 2001 *Opt. Lett.* **26** 533
[16] Iwasaki A et al 2003 *Appl. Phys.* B **76** 231
[17] Luo Q et al 2003 *Appl. Phys.* B **76** 337
[18] Hosseini S A et al 2003 *Appl. Phys.* B **77** 697
[19] Petit S et al 2000 *Opt. Commun.* **175** 323
[20] Yu J et al 2003 *Appl. Opt.* **42** 7117
[21] Vidal F et al 2000 *IEEE Trans. Plasma Sci.* **28** 418
[22] Talebpour A et al 1999 *Opt. Commun.* **163** 29
[23] Kasparian J et al 2000 *Appl. Phys.* B **71** 877
[24] Demichelis C 1969 *IEEE J. Quantum Electron.* **5** 188
[25] Vogel A et al 1999 *Appl. Phys.* B **68** 271
[26] Chin S L et al 1999 *J. Nonlinear Opt. Phys. Mater.* **8** 121
[27] Brodeur A et al 1997 *Opt. Lett.* **22** 304
[28] Kosareva G et al 1999 *J. Nonlinear Opt. Phys. Mater.* **6** 485
[29] Proulx A et al 2000 *Opt. Commun.* **174** 305
[30] Hosseini S A, Ferland B and Chin S L 2003 *Appl. Phys.* B **76** 583
[31] Hosseini S A, Yu J, Luo Q and Chin S L 2004 *Appl. Phys.* B **79** 519